Applied Catalysis B: Environmental 140–141 (2013) 412–418

Contents lists available at SciVerse ScienceDirect

Applied Catalysis B: Environmental

journal homepage: www.elsevier.com/locate/apcatb

A mechanistic study on the oxidative photodegradation of 2,6-dichlorodiphenylamine-derived drugs: Photo-Fenton *versus* photocatalysis with a triphenylpyrylium salt

P. Miró[a], A. Arques[b], A.M. Amat[b], M.L. Marin[a], M.A. Miranda[a,*]

[a] Instituto Universitario Mixto de Tecnología Química-Departamento de Química (UPV-CSIC), Avda. de los Naranjos s/n, E-46022 Valencia, Spain
[b] Grupo de Procesos de Oxidación Avanzada, Departamento de Ingeniería Textil y Papelera, Universidad Politécnica de Valencia, Campus de Alcoy Plaza Ferrándiz y Carbonell, E-03801 Alcoy, Spain

ARTICLE INFO

Article history:
Received 21 January 2013
Received in revised form 15 April 2013
Accepted 17 April 2013
Available online 23 April 2013

Keywords:
Emerging pollutants
Laser flash photolysis
Triplet
Quenching

ABSTRACT

Emerging pollutants, such as drugs, are considered a potential hazard to the environment, and therefore advanced oxidation processes are being considered candidate tools for their elimination. Here, different oxidation processes have been investigated for the degradation of the non-steroidal antiinflammatories diclofenac and meclofenamic acid, derived from the model compound 2,6-dichlorodiphenylamine. They include oxidation under photo-Fenton conditions and treatment with organic photocatalysts such as rose Bengal (RB) and triphenylpyrylium (TPP^+) salts. The role of the transient species involved in these processes (hydroxyl radical, singlet oxygen and radical cations, respectively) has been investigated by means of photophysical experiments. Based on the obtained results, participation of hydroxyl radical in photo-Fenton degradation appears feasible whereas singlet oxygen has been demonstrated to be unreactive for the degradation of the selected drugs. Finally the photocatalytic activity of triphenylpyrilium salts has been ascribed to electron transfer from the drugs to the triplet excited state of TPP^+; ground state complexes have also been observed in this case, although their contribution to the photodegradation process is only marginal.

1. Introduction

In recent years, the consumption of drugs and personal care products has increased due to our daily lifestyle [1,2]. Hence, these chemicals or their metabolites can be found in natural waters, since most of them are non-biodegradable compounds and may pass through conventional water treatment systems [3–5]. Although their concentrations in the environment are usually low, they can be considered as persistent and are currently included in the list of emerging pollutants [1]; moreover, their potential effects on aquatic ecosystems or even humans are still uncertain [6].

Photochemical processes have been demonstrated to be efficient mechanisms for the elimination of pharmaceuticals from the environment: direct or indirect photolysis is a common fate of these chemicals in natural waters, contributing to the spontaneous remediation of aqueous ecosystems [2]. In addition, photochemical oxidative processes such as photo-Fenton or solar photocatalysis have been successfully employed to treat effluents polluted with pharmaceuticals [7].

Different oxidizing species may be involved in these processes, and their actual role is still not completely established. For instance, hydroxyl radical ($OH^\bullet$) has been claimed to be the key species in the photo-Fenton process, which is based on the use of iron salts and hydrogen peroxide enhanced under UV–vis irradiation [8]. Nonetheless, the precise role of $OH^\bullet$ is still under discussion due to its difficult detection, associated with short lifetime and low steady-state concentration [9]. Some already described protocols are based on the use of chemical [10,11], fluorescent and chemoluminescent probes [12–14], or electron paramagnetic resonance (EPR) [9,15,16]. In this way, useful qualitative information has been obtained; however, the employed techniques do not always provide reliable quantitative data such as the $OH^\bullet$ reaction rate constants. Therefore time-resolved methods might be useful tools to investigate the interactions between $OH^\bullet$ and the target pollutants [17–20].

A chemical oxidation process, alternative to the photo-Fenton treatment, is based on the use of organic photocatalysts. They present absorption bands in the UV–vis region and, upon excitation, may generate transient species that can interact with the pollutants [21]. Detection of the photocatalyst-derived excited states or reactive intermediates by time-resolved techniques (emission, transient absorption spectroscopy, *etc.*) provides a powerful tool

* Corresponding author. Tel.: +34 963877807; fax: +34 963879444.
E-mail address: mmiranda@qim.upv.es (M.A. Miranda).

0926-3373/$ – see front matter © 2013 Elsevier B.V. All rights reserved.
http://dx.doi.org/10.1016/j.apcatb.2013.04.042

for the study of fast reaction kinetics. Among the organic photocatalysts, triphenylpyrilium (TPP^+) and triphenylthiapyrilium salts ($TPTP^+$) operate through an electron transfer (ET) mechanism [22], while the activity of methylene blue (MB) or rose Bengal (RB) is associated with the generation of singlet oxygen ($^1O_2$) [23].

We have previously studied the photodegradation of several pesticides both under photo-Fenton conditions and by using TPP^+ as organic photocatalyst [20]. In the former, the rate constants for reaction between $OH^\bullet$ and the pollutants are in good agreement with the experimental photodegradation results, whereas in the latter, the singlet or triplet excited states or even excited complexes have been determined to be involved in photodegradation [20,24,25].

With this background, the purpose of this paper is to perform a mechanistic study on the photocatalytic treatment of selected pharmaceuticals. For this purpose, diclofenac (DCF) has been chosen as reference compound; it is a widely employed non-steroidal anti-inflammatory drug found at relatively high concentration in waste-urban waters [26], whose environmental impact has been detected [27]. Furthermore, some studies have appeared on the photochemical fate of this drug [28] as well as on its photo-Fenton treatment [29]. With the aim of establishing structure–reactivity relationships, two structurally related compounds in which the substitution of the non-chlorinated aromatic ring is different, have also been investigated. Thus, the non-steroidal anti-inflammatory drug, meclofenamic acid (MCF, a commonly used as a pain killer) and the simple model compound 2,6-dichlorodiphenylamine (DCDPA) have been included (see Fig. 1 for structures).

Specifically, three types of oxidation conditions have been employed: (i) photo-Fenton treatment, (ii) photosensitized reaction with RB and (iii) ET-oxidation with the organic photocatalyst TPP^+. In a first stage, the effectiveness of these treatments to oxidize the selected compounds has been checked under solar simulated irradiation, and then photophysical studies have been carried out to establish the involved reaction pathways.

2. Experimental

2.1. Reagents

Diclofenac sodium salt (NaDCF), meclofenamic acid sodium salt (NaMCF), RB, TPP^+ tetrafluoroborate, NHPT, TS, naphthalene (NPT), perinaphthenone (PN), and acetonitrile were obtained from Aldrich. The model compound DCDPA was supplied by TCI Europe. Milli-Q® water was used for preparation of the aqueous solutions. All other reagents were supplied by Panreac and used without further purification.

The free acids DCF and MCF were obtained from the commercially available salts as follows: NaDCF or NaMCF (1 g) were dissolved in water (250 mL), and the corresponding solutions were acidified with diluted hydrochloric acid until acidic pH (below 3). The precipitated solids were filtered, washed and dried.

2.2. Photochemical reactions

Photochemical reactions were performed in a Luzchem photoreactor (model LZC-4V) in open Pyrex vessels with magnetic stirring, loaded with 250 mL of an aqueous solution containing a mixture of NaDCF, NaMCF and DCDPA ($C_0 = 5\ mg\ L^{-1}$ each). Irradiations were carried out under different conditions, upon addition of: (i) $10\ mg\ L^{-1}$ of iron (added as $FeSO_4{\cdot}7H_2O$) and $10\ mg\ L^{-1}$ of hydrogen peroxide, acidified to pH 3.5, (ii) RB ($10\ mg\ L^{-1}$) at pH 9 and (iii) TPP^+ ($10\ mg\ L^{-1}$) at pH 3.5. Although the pH employed is not optimal for photo-Fenton, which is 2.8, the selected conditions were chosen to avoid DCF and MCF precipitation. The selected emission maximum for the lamps (Gaussian distribution) was 350 nm, for the photocatalysis with RB, or 420 nm for photo-Fenton and photocatalytic TPP^+ treatment. These wavelengths constitute a compromise between efficient light absorption by the photocatalysts and minimization of direct substrate photolysis.

Monochromatic irradiation (558 nm) was used for MCF and RB mixtures using a Cary 300 UV–vis spectrophotometer (UV0811M209, Varian). Parallel experiments were performed using anthracene instead of MCF to confirm the reactivity with $^1O_2$ [30].

To follow the degradation kinetics, samples were taken from the reaction mixture, filtered (polypropylene filters, Teknokroma) and injected into UPLC (Perkin Elmer model Flexar UPLC FX-10 with diode-array detector, column containing oven, vacuum degasser and autosampler). A Brownlee C-18 column (30 mm × 2.1 mm, 1.9 μm particle size) was employed. The mobile phase was an isocratic mixture of formic acid (50%) and acetonitrile (50%) at the flow rate of $0.3\ mL\ min^{-1}$; the detection wavelength was fixed at 276 nm.

For detection of intermediate products in the photodegradation of DCDPA, the irradiation mixtures containing either the photocatalyst TPP^+ or the photo-Fenton reagent were concentrated by passing through a cartridge for extraction in solid phase, model Spe-edTM SPE Cartridge Amide-2, and then redissolved in 2 mL of methanol. The resulting samples were injected in a GC–MS equipment. In parallel their emission spectra were recorded to observe the possible formation of carbazole (Czl) derivative previously described in direct irradiation experiments [31,32].

2.3. Photophysical instrumentation

Quartz cells of 1 cm optical path length were employed for all photophysical measurements, which were run at room temperature in degassed acetonitrile.

Absorption spectra were recorded in a double beam Cary 300 UV–vis spectrophotometer (UV0811M209, Varian). Steady-state fluorescence spectra were recorded on a FS900 fluorometer. The absorbance of solutions at the excitation wavelength (405 nm) was kept below 0.1. Fluorescence lifetime measurements were based on single-photon-counting using a hydrogen flash lamp (1.5 ns pulse width) as excitation source.

Laser flash photolysis (LFP) studies were carried out with a Nd:YAG SL404G-10 Spectron Laser Systems using 355 nm as the excitation wavelength. The duration of single pulses was *ca.* 10 ns, and the energy was kept below 20 mJ per pulse. The detecting light source was a pulsed Lo255 Oriel Xenon lamp. The laser flash photolysis system includes the pulsed laser, the Xe lamp, a 77200 Oriel monochromator, a photomultiplier (Oriel, model 70705) system and a TDS-640A Tektronix oscilloscope. The output signal from the oscilloscope was sent to a personal computer.

2.4. Kinetic experiments to determine the reactivity of $OH^\bullet$ radical

For the kinetic experiments deaerated acetonitrile solutions containing NHPT and TS (2.9×10^{-4} M and 7.5×10^{-3} M, respectively) and different amounts of drug or standard (NPT) (up to 2.6×10^{-2} M) were submitted to LFP. The signal corresponding to the TS-$OH^\bullet$ adduct was monitored at 390 nm, whereas the signal of pyridinethiyl radical ($NHPT^\bullet$) was recorded at 490 nm to confirm the homolytic rupture.

2.5. Reactivity with $^1O_2$

The reactivity towards singlet oxygen (obtained using PN in acetonitrile as generator, absorbance = 0.3 at $\lambda_{exc} = 355$ nm) was

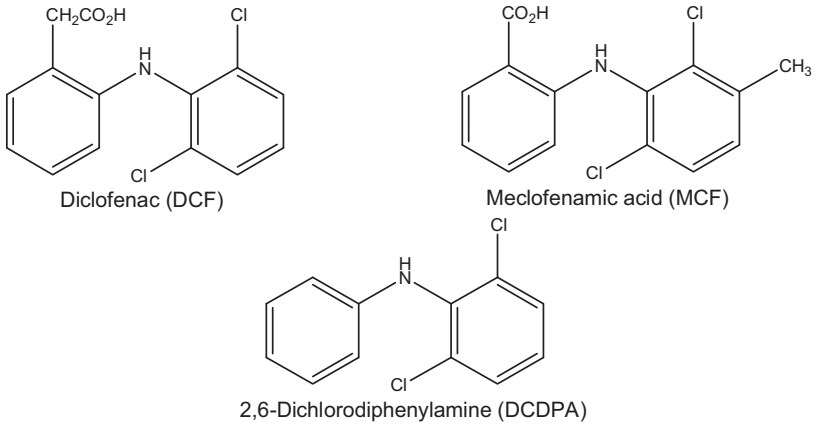

Fig. 1. Chemical structures of the selected compounds.

measured by recording the characteristic $^1O_2$ emission at 1270 nm, upon addition of increasing amounts of drug (*Q*, up to 4.6×10^{-4}, 2.8×10^{-4} and 5.2×10^{-4} M for DCF, MCF and DCDPA, respectively).

2.6. Photophysical experiments using TPP^+ as photocatalyst

For the steady-state and time-resolved fluorescence quenching experiments, increasing amounts of the drug (up to 1.28×10^{-3}, 8.68×10^{-4} and 1.28×10^{-3} M for DCF, MCF and DCDPA, respectively) were added to the corresponding deaerated TPP^+ solutions in acetonitrile.

To determine the stoichiometry of the [$TPP^{\delta+}$—$Q^{\delta'+}$] complexes, Job's plot experiments were performed, in which the absorbance changes were measured at 404 nm and plotted against drug molar fraction, keeping the total [TPP^+] + [Q] concentration constant (1×10^{-5} M).

For the LFP experiments, increasing concentrations of drug (up to 4.6×10^{-4}, 2.8×10^{-4} and 5.2×10^{-4} M for DCF, MCF and DCDPA, respectively) were added to deaerated acetonitrile solutions of TPP^+ (7×10^{-5} M). The signal of the triplet due to TPP^+ was recorded at 470 nm, and the signal corresponding to the pyranyl radical ($TPP^{\cdot}$) was registered at 550 nm.

3. Results and discussion

3.1. Photo-Fenton treatment

Photochemical oxidation of the non-steroidal anti-inflammatory drugs together with the model compound DCDPA, was evaluated under photo-Fenton conditions. Thus, a mixture of NaDCF, NaMCF and DCDPA ($C_0 = 5\ mg\ L^{-1}$ each) was treated with $FeSO_4 \cdot 7H_2O$ ($50\ mg\ L^{-1}$) and H_2O_2 ($10\ mg\ L^{-1}$) and exposed to visible light ($\lambda_{max} = 420$ nm) in acidic medium. The relative concentration of the drugs, followed by UPLC, is shown in Fig. 2. The degradation at 120 min was extensive (99% for DCF and MCF and 96% for DCDPA). For a better comparison of the reactivity of these compounds, the data obtained until 120 min were adjusted to a semi-logarithmic plot (Fig. 2, inset) leading to pseudo-first order rate constants following the order MCF $(3.9 \pm 0.2) \times 10^{-2}\ s^{-1}$ > DCF $(3.6 \pm 0.2) \times 10^{-2}\ s^{-1}$ > DCDPA $(2.4 \pm 0.1) \times 10^{-2}\ s^{-1}$.

Furthermore, GC–MS analysis of the mixtures of DCDPA was performed, and the main photoproduct found was Czl, as previously described in direct irradiations [31,32].

Next, photophysical experiments were carried out to determine the reaction of the drugs with OH•. The experiment employed for this purpose (Fig. 3) is based on the homolytic rupture of the N—O bond in the N-hydroxypyridine-2(1H)-thione (NHPT) in acetonitrile (CH_3CN) by a laser pulse of 355 nm generating the hydroxyl (OH•) and pyridinethiyl radicals ($NHPT^{\cdot}$) [18,20]; the use of *trans*-stilbene (TS) as a hydroxyl trap leads to formation of an adduct (TS-OH•) with a characteristic absorption band at 390 nm, and then the reactivity of the drugs with OH• is determined by means of competitive studies. This methodology has the advantage of checking the homolytic cleavage by detecting the pyridinethiyl radical at 490 nm.

Thus, the kinetic traces at 390 nm were recorded in the absence and in the presence of increasing amounts of DCF or DCDPA (see Fig. 4 top for DCF as an example). The intense absorption of MCF at 355 nm, acting as filter, prevented its measurement under these experimental conditions. Traces at 490 nm corresponding to the $NHPT^{\cdot}$ radical (confirming the homolytic rupture) were also recorded. The Stern–Volmer relationships were obtained by plotting the ratio between the maximum absorbance in the absence (ΔA_0) and presence (ΔA) of the drug against the drug concentration (Fig. 4, bottom). The rate constant for reaction with hydroxyl radical was obtained from the slope of the Stern–Volmer plots using naphthalene (NPT) as standard (absolute quenching rate constant, $k_{OH} = 1.8 \times 10^9\ M^{-1}\ s^{-1}$) [18,19].

From the ratio between the slopes determined for DCF or DCDPA and that for the standard NPT (Fig. 4, bottom) the quenching constants with OH• were found to be very similar, $(1.1 \pm 0.2) \times 10^9\ M^{-1}\ s^{-1}$ for DCF and $(1.0 \pm 0.1) \times 10^9\ M^{-1}\ s^{-1}$ for DCDPA. These values are far from the diffusion rate constant in acetonitrile ($k_{diff} = 1.9 \times 10^{10}\ M^{-1}\ s^{-1}$) [33] and

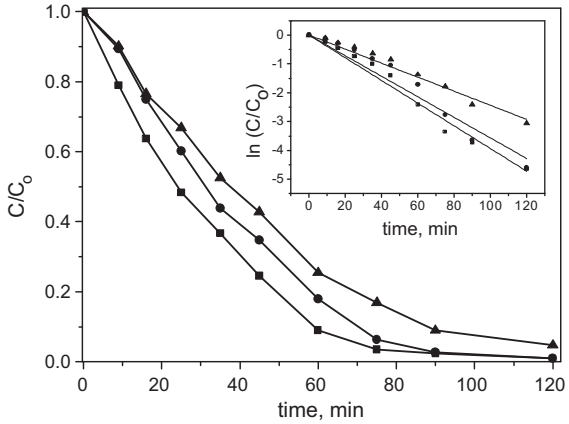

Fig. 2. Degradation C/C_0 of DCF (●), MCF (■) and DCDPA (▲) *vs* irradiation time under photo-Fenton conditions and corresponding fitting to pseudo-first order kinetic model as an inset.

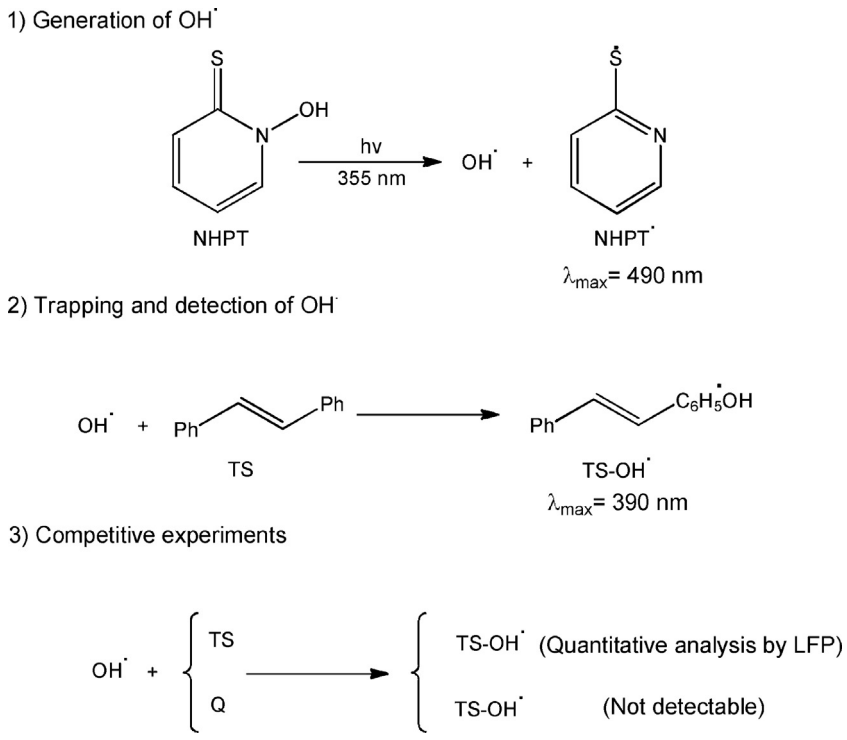

Fig. 3. Detection of OH• and quantification of its reactivity with the selected drugs (Q).

are compatible with the results obtained in photo-Fenton experiments.

3.2. Photoreactivity with $^1O_2$, using rose Bengal (RB) as generator

Photochemical degradation of the drugs using rose Bengal (RB) as organic photocatalyst was investigated. Thus, an aerated mixture of NaDCF and DCDPA (C_0 = 5 mg L^{-1} each) was treated with RB (10 mg L^{-1}), exposed to ultraviolet A light (λ_{max} = 350 nm), and the photodegradation kinetics was followed by UPLC. No photodegradation was observed even after 200 min irradiation, indicating that these compounds were not sensitive to $^1O_2$. MCF was excluded from this experiment due to its high absorbance at this wavelength. Nevertheless, a mixture of RB and MCF was subjected to monochromatic irradiation at the RB maximum (558 nm), and no changes were observed even after 100 min. In fact, although amines are well known as $^1O_2$ quenchers, rate constants depend on the substitution of the atoms in the α-position to the nitrogen since a close approach to the nitrogen atom is necessary to obtain measurable constant values [34].

Furthermore, the reactivity of $^1O_2$ with the drugs was also investigated by photophysical techniques. Thus, laser irradiation of a solution of perinaphthenone (absorbance of 0.3 at the excitation wavelength of 355 nm) led to the formation of $^1O_2$ with a characteristic emission signal at 1270 nm. This trace was recorded in the absence and in the presence of increasing concentrations of DCF and DCDPA; however, as expected from the inefficient photodegradation with RB, the signal due to $^1O_2$ kept constant even at high drug concentrations.

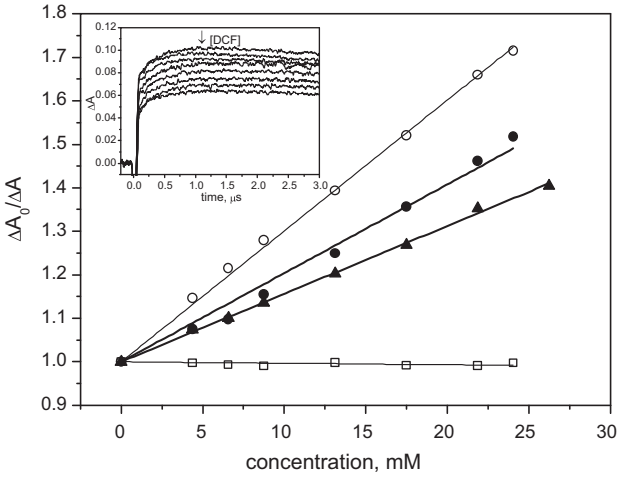

Fig. 4. Stern–Volmer plots for the generation of TS-OH• with increasing concentrations of the standard NPT (○), DCF (●) and the model compound DCDPA (▲) *vs* drug concentration. The Stern–Volmer plot for the signal of NPTH• recorded at 490 nm is also shown (□). Inset: kinetic traces obtained at 390 nm in laser flash photolysis (355 nm) upon addition of increasing concentrations of DCF to a mixture of NHPT and TS.

3.3. Photodegradation using triphenylpyrylium (TPP$^+$) as electron transfer photocatalyst

The effectiveness of TPP$^+$ as homogeneous organic photocatalyst acting mainly by an electron transfer mechanism was tested in the photodegradation of the drugs. Thus, a mixture of NaDCF, NaMCF and DCDPA (C_0 = 5 mg L^{-1} each) was treated with TPP$^+$ (10 mg L^{-1}) and exposed to the light of a photoreactor (λ_{max} = 420 nm). The photodegradation kinetics was analyzed by UPLC. Again in this case, the relative drug concentration was adjusted to a semi-logarithmic plot (Fig. 5), and the order of reactivity from the obtained pseudo-first order rate constants was: DCF, $(2.1 \pm 0.2) \times 10^{-2}$ s^{-1} > DCDPA, $(1.7 \pm 0.1) \times 10^{-2}$ s^{-1} > MCF, $(3.4 \pm 1.3) \times 10^{-3}$ s^{-1}.

The emission (λ_{exc} = 260 nm) and the corresponding excitation spectra of the photoirradiated DCDPA (in the presence of TPP$^+$) were completely coincident to those of Czl, unambiguously demonstrating that Czl is indeed formed as the main photoproduct.

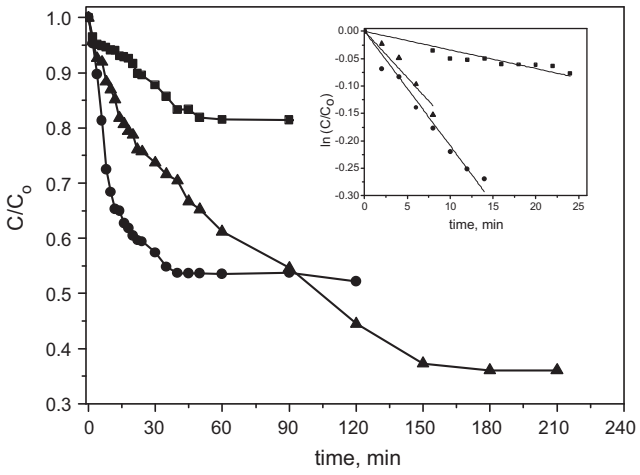

Fig. 5. Degradation C/C_0 of DCF (●), MCF (■) and DCDPA (▲) *vs* irradiation time using TPP^+ as homogeneous photocatalyst; inset: corresponding fitting to pseudo-first order kinetic model.

3.4. Fluorescence quenching studies

Photophysical experiments were carried out in order to determine the reactive species responsible for the photocatalytic activity of TPP^+.

First, the possible involvement of the singlet excited state of TPP^+ was evaluated by means of fluorescence experiments. Thus, when the steady-state emission spectrum of TPP^+ in deaerated acetonitrile solutions (λ_{exc} = 405 nm) was recorded upon addition of increasing concentrations of the drugs, a decrease of the intensity was observed in all cases (see Fig. 6 for DCDPA as an example). Then, by application of the Stern–Volmer relationship (Fig. 6, inset) and using the already reported singlet lifetime of TPP^+ (4.2 ns) [35] the corresponding quenching rate constants were determined: MCF, $(3.0 \pm 0.1) \times 10^{11}\ M^{-1}\ s^{-1}$ > DCDPA, $(8.4 \pm 0.2) \times 10^{10}\ M^{-1}\ s^{-1}$ > DCF $(6.3 \pm 0.2) \times 10^{10}\ M^{-1}\ s^{-1}$.

The active involvement of the singlet excited state was also evaluated by means of time-resolved emission spectroscopy. However, conversely to the steady-state results, the singlet lifetime of TPP^+ remained constant after addition of increasing amounts of the drugs. This fact, together with the determined values for the quenching rate constants above the diffusion rate in CH_3CN ($k_{diff} = 1.9 \times 10^{10}\ M^{-1}\ s^{-1}$), pointed to the formation of ground-state complexes as the species responsible, at least in part, for the observed fluorescence quenching.

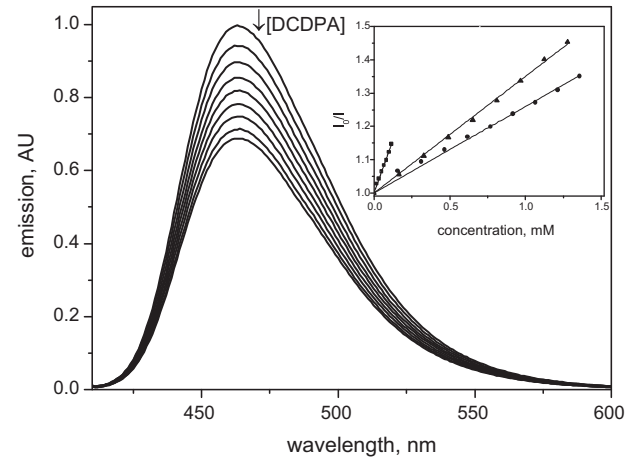

Fig. 6. Fluorescence spectra of TPP^+ in deaerated acetonitrile (λ_{exc} = 405 nm) recorded in the presence of increasing amounts of DCDPA ($(0–1.3) \times 10^{-3}$ M) as a representative example; inset: Stern–Volmer plots obtained for the fluorescence quenching of TPP^+ by DCF (●), MCF (■) and DCDPA (▲) (λ_{exc} = 405 nm).

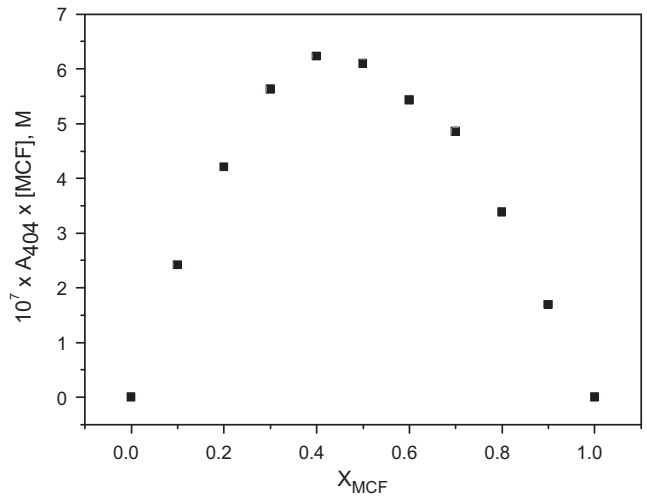

Fig. 7. UV absorption Job's plot for TPP^+ against MCF molar fraction, at total concentration ($[TPP^+] + [MCF]$) of 50 μM.

3.5. Formation of ground state complexes

Job's plot experiments were performed to check the possible formation of ground-state complexes [36,37], based on the absorbance changes of the UV–vis spectrum of different solutions of constant ($[TPP^+] + [Q]$) concentration (1×10^{-5} M in acetonitrile). Thus, the absorbance at 404 nm was plotted *vs* molar fraction of drug; the obtained Job's plots with a maximum at $X_{drug} = 0.5$ indicated a 1:1 stoichiometry for all three cases (see Fig. 7 for MCF as an example),

$$TPP^+ + Q \overset{K}{\rightleftarrows} [TPP^{\delta+} - Q^{\delta'+}] \quad (1)$$

$$K = \frac{[TPP^{\delta+} - Q^{\delta'+}]}{[TPP^+][Q]} \quad (2)$$

where Q represents DCF, MCF or DCDPA and K is the complexation constant which was determined by applying the Benesi–Hildebrand relationship [38,39]

$$\frac{1}{I_0 - I} = \frac{1}{I_0 - I_1} + \frac{1}{(I_0 - I_1)K[Q]} \quad (3)$$

where I_0, I and I_1 are the emission intensities in the absence, after every addition and at infinite concentration of the drug, respectively. The K values were obtained from the slope and intercept of the linear fittings and resulted to be MCF, $(442 \pm 14)\ M^{-1}$ > DCDPA, $(307 \pm 7)\ M^{-1} \approx$ DCF, $(304 \pm 10)\ M^{-1}$.

3.6. Transient absorption spectroscopy

The possible involvement of the triplet excited state of TPP^+ in an electron transfer mechanism was investigated by laser flash photolysis (LFP) experiments. Thus, excitation (λ_{exc} = 355 nm) of a deaerated solution of TPP^+ in acetonitrile (7×10^{-5} M) led to a broad absorption band (400–800 nm) assigned to the triplet state [22]. Then, the lifetime of the signal monitored at 470 nm was analyzed upon addition of increasing concentrations of the drugs (up to 4.6×10^{-4} M, 2.8×10^{-4} M and 5.2×10^{-4} M for DCF, MCF and DCDPA, respectively). A sharp decrease in the triplet lifetime was observed for the three drugs, concomitant with an increase of the signal at 550 nm due to the pyranyl radical ($TPP^{\bullet}$, the semireduced

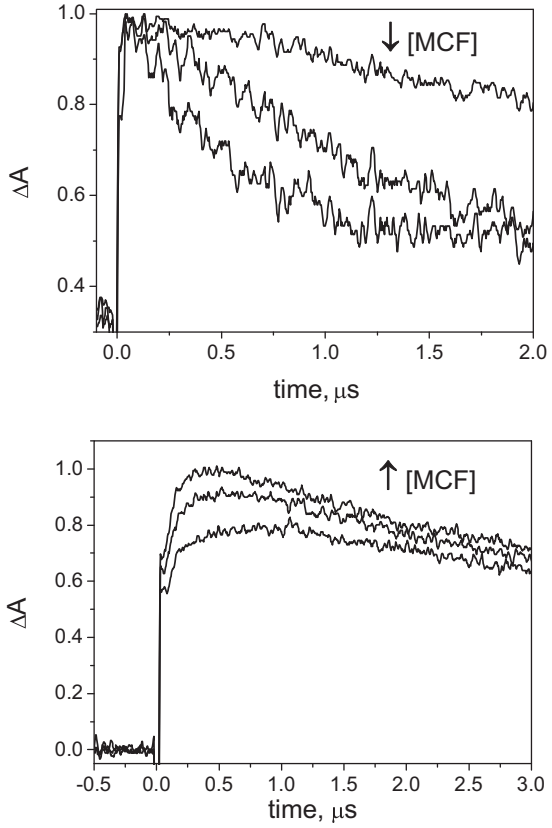

Fig. 8. Kinetic traces obtained upon irradiation (λ_{exc} = 355 nm) of deaerated acetonitrile solutions of TPP^+ (7×10^{-5} M) in the presence of increasing concentrations of MCF ((0–2.8) × 10^{-4} M) as an example. Top: decay of the TPP^+ triplet state recorded at 470 nm, bottom: growth and decay of $TPP^{\bullet}$ recorded at 550 nm.

species arising from TPP^+) as a proof of the photoinduced electron transfer process (see Figure 8 for MCF as an example); the corresponding drug radical cations were not observed in the available spectral window (300–700 nm). The shortening of the triplet lifetime was adjusted to a Stern–Volmer relationship; the quenching rate constants, estimated from the slope of the corresponding linear fittings, were: $(2.6 \pm 0.1) \times 10^{10}$ M^{-1} s^{-1}, $(2.5 \pm 0.1) \times 10^{10}$ M^{-1} s^{-1} and $(1.9 \pm 0.1) \times 10^{10}$ M^{-1} s^{-1}, for MCF, DCDPA and DCF, respectively.

The feasibility of photoinduced electron transfer involving the triplet excited state of TPP^+ was demonstrated using the Rehm–Weller equation [40]:

$$\Delta G(\text{kcal mol}^{-1}) = 23.06\,[E_{ox}(Q) - E_{red}(TPP^+)] - E_T^*(TPP^+) \qquad (4)$$

The values for $E_{red}(TPP^+)$ and $E_T^*(TPP^+)$ were taken from the literature (−0.29 V *vs.* SCE and 53 kcal mol^{-1}, respectively) [22,41,42]. Using the reported E_{ox}(DCF) of +0.89 V (*vs.* SCE), [43] the estimated ΔG was −26 kcal mol^{-1} indicating that electron transfer from DCF to the triplet excited state of TPP^+ is indeed exergonic. Although the oxidation potentials of MCF or DCDPA were not found in the literature, they should be similar to that of DCF, as inferred from their chemical structure; therefore the process should be exergonic in all cases.

3.7. Mechanistic proposal

Photodegradation of the drugs in the presence of TPP^+ has been observed in the three cases, with a pseudo-first order rate constant following the order DCF > DCDPA > MCF. This does not correlate well with the relative reactivities observed under photo-Fenton conditions, indicating that $OH^{\bullet}$ does not play a major role in TPP^+ mediated photodegradation. Formation of ground-state complexes between the photocatalyst and the drugs has been demonstrated (from the steady-state fluorescence quenching, Job's plots and Benesi–Hildebrand treatment). Nevertheless, the active participation of the singlet excited state can be disregarded, since no changes in the fluorescence lifetime have been observed in the presence of the drugs. By contrast, the decrease in the triplet lifetime upon addition of the drugs points to an active participation of the triplet. Furthermore, thermodynamic considerations (Rehm–Weller) and formation of the reduced species ($TPP^{\bullet}$) after laser irradiation in the presence of the drugs, strongly support the involvement of a photoinduced electron transfer process (Scheme 1).

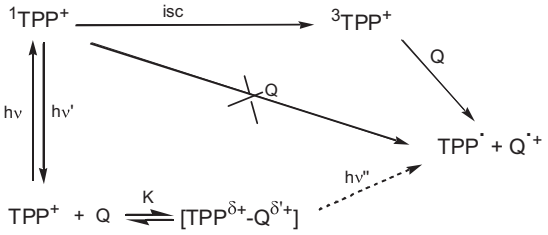

Scheme 1. Mechanism proposed for the photodegradation of the drugs by TPP^+.

Considering the concentrations of DCF (1.7×10^{-5} M), MCF (1.7×10^{-5} M), DCDPA (2.1×10^{-5} M), and photocatalyst TPP^+ (2.5×10^{-5} M) employed in the photochemical reactions and taking into account the complexation constants (K), the concentration of ground state complex [$TPP^{\delta+}$–$Q^{\delta'+}$] was obtained from Eq. (2) and found to be very low in all cases. Indeed, less than 1% of the initial TPP^+ should be forming the complex under these experimental conditions.

By contrast, most of the TPP^+ excited triplet state should be quenched by DCF, MCF and DCDPA; rough calculations based on the kinetic parameters (τ_T, k_q) and the concentration of the three compounds indicate that *ca.* 30% of the photons initially absorbed by TPP^+ follow the electron transfer pathway.

4. Conclusions

Photodegradation of DCF, MCF and DCDPA has been achieved under photo-Fenton oxidation conditions and also by treatment in the presence of TPP^+ as organic photocatalyst. In the former case, the order of reactivity is MCF > DCF > DCDPA, whereas in the latter the relative reactivity is DCF > DCDPA > MCF. Photophysical experiments confirm the feasibility of $OH^{\bullet}$ as the species responsible for photodegradation; conversely, electron transfer from the triplet excited state of TPP^+ is the predominant mechanism involved in this photocatalytic degradation. A qualitative correlation between the chemical structure of the studied compounds and the key step involved in the photodegradation can also be made. On one hand, in agreement with the photo-Fenton results, the carboxyl group of MCF would stabilize the intermediate obtained after the hydroxyl radical attack. On the other hand, the substitution of the non-chlorinated aromatic ring agrees well with the observed trend in the one-electron oxidation by TPP^+. Thus, the pseudo-first order rate constants follow the order DCF > DCDPA > MCF as passing from an electron-donating (—CH_2R) to a non-substituted and then to an electron-withdrawing (—CO_2R) substituent.

Acknowledgements

Financial support from the Spanish Government (Projects CTQ2009-13699 and CTQ2009-13459-C05-03) and Technical University of Valencia (Programa de Apoyo a la Investigacion y

Desarrollo 2775 and Predoctoral FPI fellowship for P. Miró) are gratefully acknowledged.

References

[1] D. Barcelo (Ed.), The Handbook of Environmental Chemistry: Emerging Organic Pollutants in Waste Waters and Sludge, vol. 2, Springer-Verlag, Berlin, Heidelberg, 2005.
[2] S.K. Khetan, T.J. Collins, Chemical Reviews 107 (2007) 2319–2364.
[3] D. Barcelo, M. Petrovic, Analytical and Bioanalytical Chemistry 385 (2006) 983–984.
[4] D. Barcelo, M. Petrovic, TRAC Trends in Analytical Chemistry 25 (2006) 191–193.
[5] S. Rodriguez-Mozaz, M.J. Lopez de Alda, D. Barcelo, Talanta 69 (2006) 377–384.
[6] K.E. Murray, S.M. Thomas, A.A. Bodour, Environmental Pollution 158 (2010) 3462–3471.
[7] S. Malato, P. Fernandez-Ibanez, M.I. Maldonado, J. Blanco, W. Gernjak, Catalysis Today 147 (2009) 1–59.
[8] J.J. Pignatello, E. Oliveros, A. MacKay, Critical Reviews in Environmental Science and Technology 36 (2006) 1–84.
[9] Y. Luo, X.-r. Wang, L.-l. Ji, Y. Su, Journal of Hazardous Materials 171 (2009) 1096–1102.
[10] D. Vione, G. Falletti, V. Maurino, C. Minero, E. Pelizzetti, M. Malandrino, R. Ajassa, R.I. Olariu, C. Arsene, Environmental Science and Technology 40 (2006) 3775–3781.
[11] N. Nakatani, N. Hashimoto, H. Shindo, M. Yamamoto, M. Kikkawa, H. Sakugawa, Analytica Chimica Acta 581 (2007) 260–267.
[12] S. Yamaguchi, N. Kishikawa, K. Ohyama, Y. Ohba, M. Kohno, T. Masuda, A. Takadate, K. Nakashima, N. Kuroda, Analytica Chimica Acta 665 (2010) 74–78.
[13] N. Soh, Analytical and Bioanalytical Chemistry 386 (2006) 532–543.
[14] T. Maki, N. Soh, T. Fukaminato, H. Nakajima, K. Nakano, T. Imato, Analytica Chimica Acta 639 (2009) 78–82.
[15] G.R. Buettner, R.P. Mason, Methods in Enzymology 186 (1990) 127–133.
[16] A. Nakajima, M. Tahara, Y. Yoshimura, H. Nakazawa, Journal of Photochemistry and Photobiology A: Chemistry 174 (2005) 89–97.
[17] B.M. Aveline, I.E. Kochevar, R.W. Redmond, Journal of the American Chemical Society 118 (1996) 289–290.
[18] M.P. DeMatteo, J.S. Poole, X. Shi, R. Sachdeva, P.G. Hatcher, C.M. Hadad, M.S. Platz, Journal of the American Chemical Society 127 (2005) 7094–7109.
[19] J.S. Poole, X. Shi, C.M. Hadad, M.S. Platz, Journal of Physical Chemistry A 109 (2005) 2547–2551.
[20] M.L. Marin, V. Lhiaubet-Vallet, L. Santos-Juanes, J. Soler, J. Gomis, A. Argues, A.M. Amat, M.A. Miranda, Applied Catalysis B: Environmental 103 (2011) 48–53.
[21] M.L. Marin, L. Santos-Juanes, A. Arques, A.M. Amat, M.A. Miranda, Chemical Reviews 112 (2012) 1710–1750.
[22] M.A. Miranda, H. Garcia, Chemical Reviews 94 (1994) 1063–1089.
[23] D. Gryglik, J.S. Miller, S. Ledakowicz, Journal of Hazardous Materials 146 (2007) 502–507.
[24] M.L. Marin, A. Miguel, L. Santos-Juanes, A. Arques, A.M. Amat, M.A. Miranda, Photochemical and Photobiological Sciences 6 (2007) 848–852.
[25] A. Arques, A.M. Amat, L. Santos-Juanes, R.F. Vercher, M.L. Marín, M.A. Miranda, Catalysis Today 144 (2009) 106–111.
[26] J. Hartmann, P. Bartels, U. Mau, M. Witter, W.V. Tumpling, J. Hofmann, E. Nietzschmann, Chemosphere 70 (2008) 453–461.
[27] B. Hoeger, B. Kollner, D.R. Dietrich, B. Hitzfeld, Aquatic Toxicology 75 (2005) 53–64.
[28] J.L. Packer, J.J. Werner, D.E. Latch, K. McNeill, W.A. Arnold, Aquatic Sciences 65 (2003) 342–351.
[29] L.A. Perez-Estrada, S. Malato, W. Gernjak, A. Aguera, E.M. Thurman, I. Ferrer, A.R. Fernandez-Alba, Environmental Science and Technology 39 (2005) 8300–8306.
[30] A.E. Gekhman, A.P. Makarov, V.M. Nekipelov, E.P. Talzi, O.Y. Polotnyuk, K.I. Zamaraev, I.I. Moiseev, Bulletin of the Academy of Sciences of the USSR, Division of Chemical Science 34 (1985) 1545.
[31] S. Encinas, F. Bosca, M.A. Miranda, Photochemistry and Photobiology 68 (1998) 640–645.
[32] S. Encinas, F. Bosca, M.A. Miranda, Chemical Research in Toxicology 11 (1998) 946–952.
[33] S.L. Murov, I. Carmichael, G.L. Hug, Handbook of Photochemistry, 2nd ed., M. Dekker, New York, 2009.
[34] B.M. Monroe, Journal of Physical Chemistry 81 (1977) 1861–1864.
[35] F. Morlet-Savary, S. Parret, J.P. Fouassier, K. Inomata, T. Matsumoto, Journal of the Chemical Society-Faraday Transactions 94 (1998) 745–752.
[36] C.Y. Huang, in: L.P. Daniel (Ed.), Methods in Enzymology, vol. 87, Academic Press, San Diego, CA, 1982, pp. 509–525.
[37] P. Maccarthy, Analytical Chemistry 50 (1978) 2165.
[38] S. Nigam, G. Durocher, Journal of Physical Chemistry 100 (1996) 7135–7142.
[39] H.A. Benesi, J.H. Hildebrand, Journal of the American Chemical Society 71 (1949) 2703–2707.
[40] D. Rehm, A. Weller, Israel Journal of Chemistry 8 (1970) 259–271.
[41] M. Martiny, E. Steckhan, T. Esch, Chemische Berichte-Recueil 126 (1993) 1671–1682.
[42] R. Searle, J.L. Williams, D.E. Demeyer, J.C. Doty, Chemical Communications (1967) 1165.
[43] F. Manea, M. Ihos, A. Remes, G. Burtica, J. Schoonman, Electroanalysis (New York) 22 (2010) 2058–2063.